# Dynamic analysis by FEM of blast-induced ground vibrations

Caroline B. Zorzal[1], Christianne de L. Nogueira[1]

[1]*Programa de Pós Graduação em Engenharia Mineral, Universidade Federal de Ouro Preto*
*Campus Universitário, Morro do Cruzeiro, Ouro Preto/MG 35400-000, Brazil.*
*carolinezorzal@gmail.com, chris@ufop.edu.br*

**Abstract.** Peak particle velocities (PPV) are fundamental for understanding and managing blast-induced ground vibration levels and their impact on neighboring structures. Given that the numerical analysis of seismic vibrations has been revealed as a method that may substantially contribute to estimating PPV levels, this research employs a numerical approach using the finite element method (FEM) to evaluate blast-induced ground vibration in rock masses. A dynamic module of the stress-strain analysis was developed in ANLOG software based on the FEM displacement formulation to estimate the variations of displacement, strain, and stress induced by blasting. Since Rayleigh damping coefficients are frequently used in FEM analysis to model the effect of physical damping in geological mediums, a study was conducted to determine the effect of Rayleigh coefficients on the PPV numerical attenuation law. After understanding the influence of the Rayleigh coefficients on the results, the PPV numerical attenuation law is obtained using ANLOG. It shows good agreement with values estimated by empirical methods and numerical results available in the specialized literature.

**Keywords:** blasting, elastic wave propagation, dynamic equilibrium, finite element method, Rayleigh coefficients.

## 1 Introduction

In rock blasting, the controlled release of energy from the explosive is primarily intended to fragment and extract the rock mass. However, part of this energy is also responsible for generating undesirable effects. Among these, seismic ground vibrations stand out for their potential to affect the well-being of the surrounding population, as well as the stability and integrity of the rock mass and structures such as dams, waste piles, civil constructions, and others.

Peak particle velocity (PPV) is a commonly used parameter in the minerals industry for quantifying and evaluating the damage potential of seismic vibrations. Seismographs measure particle vibration velocity in three orthogonal components: vertical, transverse, and longitudinal or radial. In turn, the PPV is defined as the highest value obtained among all values measured in all vibration velocity components over a given time interval (ABNT NBR 9653 [1]). Several alternative initiatives have been taken, over time, in order to estimate the PPV levels generated from rock blasting. Empirical, statistical, mathematical, and advanced computational techniques have been developed and have shown to be valuable tools for studying and controlling vibration levels.

The Finite Element Method (FEM) has been widely used in the estimation of seismic vibrations induced by blasting, either individually or in coupled with other methods. The numerical approach via FEM allows tracking the propagation of seismic waves through the rock mass in time and space, facilitating analysis of its response to the dynamic efforts generated. The method has shown to be efficient in dealing with complicated geometries and various heterogeneities in the geological context (Semblat [2]). Furthermore, when compared to traditional empirical approaches and data acquired in situ, numerous research have demonstrated excellent results (Ma et al. [3]; Toraño et al. [4]; Jommi e Pandolfi [5]; Lu et al. [6]; Liu et al. [7]; Xu et al. [8]).

In this context, numerical analysis of seismic vibrations via FEM is revealed as an approach that may substantially contribute to the knowledge and control of blast-induced ground vibrations. Therefore, the goal of this research is to use a numerical approach to assess the seismic vibrations produced by blasting. A dynamic stress-strain analysis module was developed in the open-source computer program ANLOG (Zorzal [9]) using the finite element approach based on a displacement formulation to estimate the variations in displacement, velocity, and stress fields generated by blasting.

ANLOG was then used in an application example in a limestone quarry in Spain to predict seismic vibrations caused by blasting. In order to obtaining the PPV numerical attenuation law, the peak particle velocity values obtained from ANLOG was plotted as a function of the scaled distance (D) defined as (ABNT NBR 9653 [1]):

$$D = \frac{R}{\sqrt{Q}}, \tag{1}$$

where R is the distance between blast and monitoring point and Q is the maximum charge per delay. The numerical attenuation curve is generated from a study to examine the impact of the Rayleigh coefficients, and it is compared to the attenuation law reported by Toraño et al. [4] based on in-situ measured data.

## 2 Mathematical and numerical formulation of the dynamic analysis

The system of motion equations that govern a seismic wave that propagates in an infinite, homogenous, and isotropic medium with perfect elasticity can be represented as:

$$\nabla^{T}\left(\mathbf{D}\nabla\mathbf{u}\right) - \mathbf{f}_{B} + \rho\ddot{\mathbf{u}} = \mathbf{0}, \tag{2}$$

where $\nabla$ is a differential operator; $\mathbf{D}$ is the constitutive matrix that depends on elastic properties; $\rho$ is the material density of the medium; u and ü are displacement and acceleration vectors; and $\mathbf{f_B}$ is the body force vector.

Equation (2) must be satisfied in the problem domain (V) and at all time instants (t) of the analysis. Equation (2) also must obey the following boundary and initial conditions (Martins [10]):

$$\boldsymbol{\sigma}\mathbf{n} = \mathbf{f}_{S} \text{ in } S_q, \tag{3a}$$

$$\mathbf{u}_{i} = \boldsymbol{\delta}_{i} \text{ in } S_u, \tag{3b}$$

$$\mathbf{u}\left(\mathbf{x},0\right) = \mathbf{u}_{0}\left(\mathbf{x}\right) \text{ in V, and} \tag{3c}$$

$$\dot{\mathbf{u}}\left(\mathbf{x},0\right) = \dot{\mathbf{u}}_{0}\left(\mathbf{x}\right) \text{ in V,} \tag{3d}$$

where $S_q$ and $S_u$ are, respectively, the problem boundary with prescribed force and displacement; $\mathbf{f}_S$ is the surface vector; $\boldsymbol{\delta}_i$ is the prescribed displacement; and $\mathbf{u}_0$ and $\dot{\mathbf{u}}_0$ are the initial displacements and velocities.

The differential equation system described by eq. (2) may be stated in the finite element domain ($V_e$) as a function of the nodal displacement, velocities and acceleration vectors ($\hat{\mathbf{u}}, \hat{\dot{\mathbf{u}}}$ and $\hat{\ddot{\mathbf{u}}}$), according to the FEM displacement isoparametric formulation, as:

$$\mathbf{M}_{e}\hat{\ddot{\mathbf{u}}} + \mathbf{C}_{e}\hat{\dot{\mathbf{u}}} + \mathbf{K}_{e}\hat{\mathbf{u}} = \mathbf{F}_{e}, \tag{4}$$

where $\mathbf{M}_e$, $\mathbf{C}_e$ and $\mathbf{K}_e$ are, respectively, the mass, damping and stiffness elementary matrices and $\mathbf{F}_e$ is the elementary external load vector. Taking into account the global arrangement of all elementary matrices, the equation of global equilibrium may be defined as:

$$\mathbf{M}\hat{\ddot{\mathbf{U}}} + \mathbf{C}\hat{\dot{\mathbf{U}}} + \mathbf{K}\hat{\mathbf{U}} = \mathbf{F}, \tag{5}$$

where $\mathbf{M}$, $\mathbf{C}$ and $\mathbf{K}$ are, respectively, the mass, damping and stiffness global matrices; $\mathbf{F}$ is the global external load vector; and $\hat{\ddot{\mathbf{U}}}$, $\hat{\dot{\mathbf{U}}}$ and $\hat{\mathbf{U}}$ are, respectively, the global nodal acceleration, velocity and displacement vectors.

In geomechanical applications, it is usual consider the effect of physical damping by using the Rayleigh damping coefficients ($\alpha_R$ and $\beta_R$). In this case, the damping matrix $\mathbf{C}$ may be obtained as a linear combination of the mass ($\mathbf{M}$) and the stiffness ($\mathbf{K}$) matrix, as follow:

$$\mathbf{C} = \alpha_{R}\mathbf{M} + \beta_{R}\mathbf{K} \tag{6}$$

The Rayleigh coefficients $\alpha_R$ and $\beta_R$ may be estimated, respectively, by (Chopra [15]; Clough and Penzien [13]):

$$\alpha_R = \xi \frac{2\omega_i\omega_j}{\omega_i + \omega_j} \tag{7a}$$

$$\beta_R = \xi \frac{2}{\omega_i + \omega_j} \tag{7b}$$

where $\omega_i$ and $\omega_j$ are the natural frequencies referring, respectively, to the $i^{th}$ and $j^{th}$ vibration modes; and $\xi$ is the damping ratio for both vibration modes.

To solve the dynamic equilibrium equation system, eq. (5), ANLOG uses the Newmark method of direct integration, whose implicit algorithm is given by Bathe [11]. The parameters $\delta$ and $\alpha$ are used in this approach to determine the accuracy and stability of the solution (Bathe [11]).

# 3 Examples

## 3.1 Verification problem

The aim of this example is to validate the dynamic modulus implemented in ANLOG by solving a one-dimensional problem of wave propagation in a homogeneous and elastic medium, without dissipative forces. This verification example assesses the displacements and velocities variations, in time and space, experienced by a cantilever beam (Fig. 1) under a Heaviside loading, p(t), defined as:

$$p(t) = P_0 H(t)\text{, with } H(t) = \begin{cases} 0, & t < 0 \\ 1, & t \geq 0 \end{cases}, \tag{8}$$

where $P_0$ is the load magnitude, adopted as -10 kN. The beam measures 0.5m in length (L), 0.01m in height (h), and 0.01m in width (e). With a Young modulus (E) of 200 GPa and a density ($\rho$) of 8t/m$^3$, the beam material exhibits linear elastic behavior and null characteristic damping.

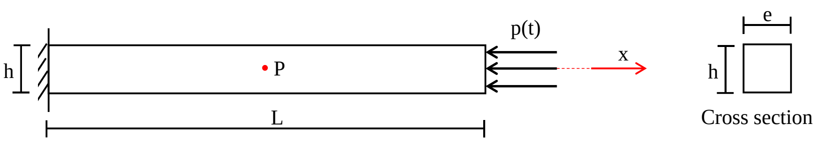


Figure 1: Cantilever beam under Heaviside load.

According to Clough and Penzien [12], the analytical solution to this problem in terms of displacement and velocity can be determined from the following equations:

$$u(x,t) = \frac{8P_0L}{\pi^2 EA} \sum_{n=1}^{\infty} \left\{ \frac{(-1)^{n-1}}{(2n-1)^2} \operatorname{sen}\left( \frac{2n-1}{2} \frac{\pi x}{L} \right) \left[ 1 - \cos\left( \frac{2n-1}{2L} \pi c t \right) \right] \right\} \text{ and} \tag{9a}$$

$$v(x,t) = \frac{8P_0L}{\pi^2 EA} \sum_{n=1}^{\infty} \left\{ \frac{(-1)^{n-1}}{(2n-1)^2} \operatorname{sen}\left( \frac{2n-1}{2} \frac{\pi x}{L} \right) \left[ \left( \frac{2n-1}{2L} \pi c \right) \operatorname{sen}\left( \frac{2n-1}{2L} \pi c t \right) \right] \right\}, \tag{9b}$$

where c is the wave velocity, defined as 5000 m/s² for the analyzed material.

This problem was solved numerically with the ANLOG program, using the Newmark algorithm considering: $\delta$ of 0.5; $\alpha$ of 0.25; $\Delta t$ of 1.0x10$^{-3}$ms; and final time of analysis of 1 ms. The adopted finite element mesh consists in 50 quadrilateral quadratic elements (Q8 element, Nogueira [13]) of the same size and 253 nodal points.

Figure 3 depicts the analytical (Clough and Penzien, 1993) and numerical (ANLOG) results in terms of displacements and velocities obtained at point P in the center of the beam (Fig. 1). The ANLOG results in terms of the displacement are in a good agreement with the analytical solution (Fig. 2a). On the other hand, the numerical velocity results demonstrate a high degree of variability around the analytical answers (Fig. 2b).

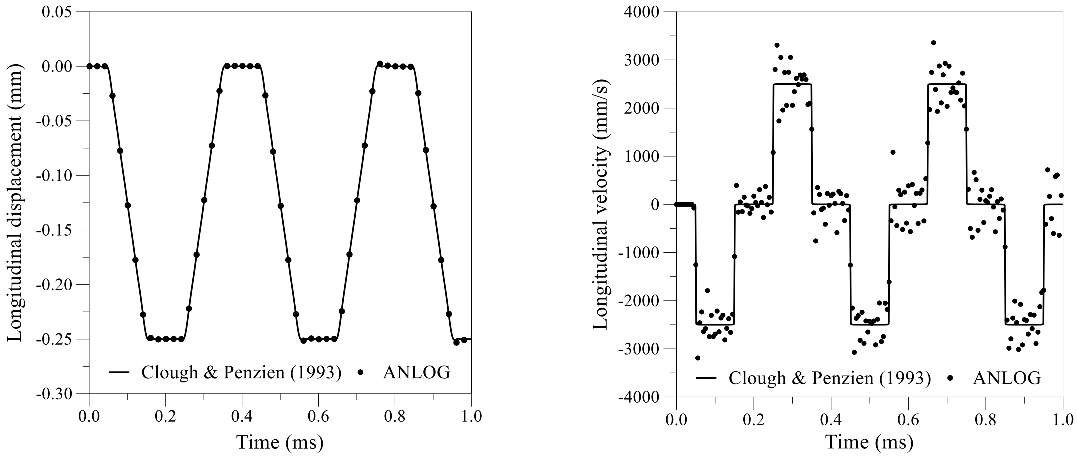


a) Displacement (mm) b) Velocity (mm/s)

Figure 2. Evolution in time of the (a) displacement and (b) velocity at point P.

In order to produce a more steady and precise numerical answer, the values of the time integration parameters (δ and α) of the Newmark algorithm were changed from the above-mentioned values. As can be observed in Fig. 3, the noise generated during wave propagation is minimized when the values 0.625 and 0.316 are used for δ and α, respectively and the results obtained are satisfactory for both the primary variable (displacement) and the secondary variable (velocity). We may conclude from the investigated example that the computational implementation into ANLOG was successful in providing solutions that agreed with the analytical results.

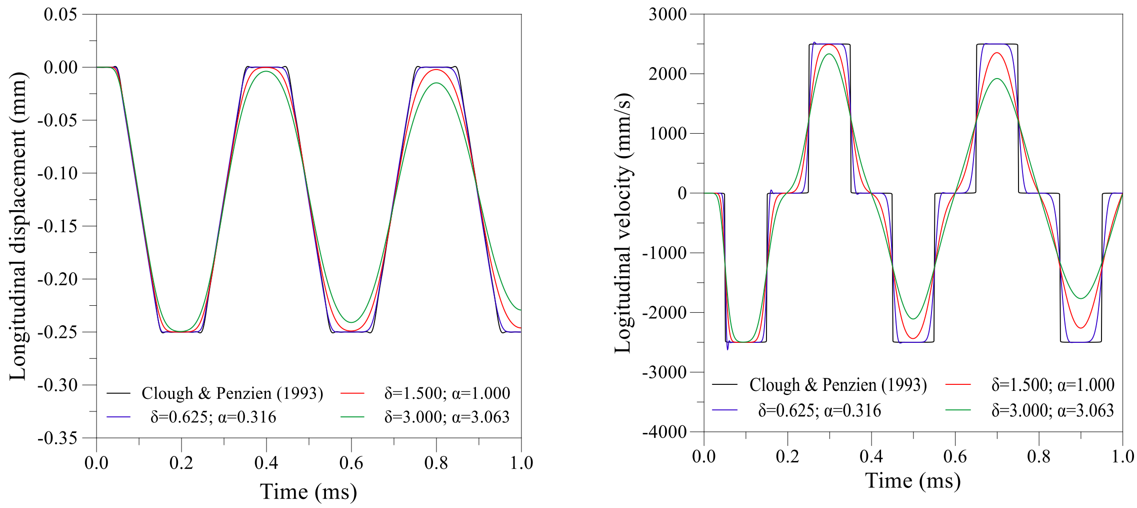


a) Displacement (mm) b) Velocity (mm/s)

Figure 3. Influence of the time integration parameters of Newmark algorithm.

### 3.2 Application problem

In this application example, ANLOG is used to estimate seismic vibrations induced by blasting in a rock mass consisting of limestone with density (ρ) of 2.6t/m$^3$, elasticity module (E) of 12GPa, and Poisson coefficient (ν) of 0.2. The PPV values obtained from ANLOG [14] are compared with the in-situ results obtained by Toraño et al. [4] in a limestone quarry located near an urbanized area in Spain.

The charge of 100Kg of explosives were loaded into the 20m deep blasthole, which also corresponds to the bench height ($H_B$). Toraño et al. [4] estimated that the blasting creates a peak borehole pressure ($P_B$) of 28MPa in the blasthole wall. The dynamic load that reflects the detonation pressure pulse function is modeled in this study by considering the optimized pressure-time profile proposed by Saharan and Mitri [14] for non-ideal detonation in 38 mm diameter blasthole on hard brittle rocks (Fig. 4). The description of this pressure pulse depends on normalized pressure (the ratio of applied pressure to peak borehole pressure) values at different time instants.

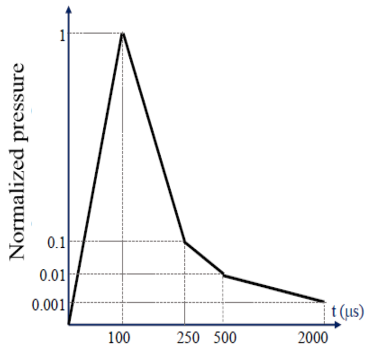


Fig. 4 Non-ideal detonation optimized pressure time profile (Saharan and Mitri [14]).

The problem, which is evaluated in plane strain, has the finite element mesh and boundary conditions depicted in Fig. 5. The study area has a length (L) of 600m by 150m in depth (H). These values were arbitrated to prevent the development of spurious wave reflections in the model's contours. The finite element mesh consists of 396 quadratic elements of eight nodes (Q8 element, Nogueira [13]) and 1289 nodes. The sizes of the elements vary from (5x5)m near the point of application of the detonation charge to (50x50)m at the most distant points. The peak particle velocity values were collected at the surface points $P_1$, $P_2$, $P_3$, $P_4$, $P_5$, $P_6$, $P_7$, $P_8$, $P_9$, $P_{10}$, $P_{11}$, $P_{12}$, $P_{13}$ and $P_{14,}$ respectively, at 30, 50, 75, 125, 150, 175, 200, 250, 300, 350, 400, 450 and 500m distant from the blasting front (Fig. 5).

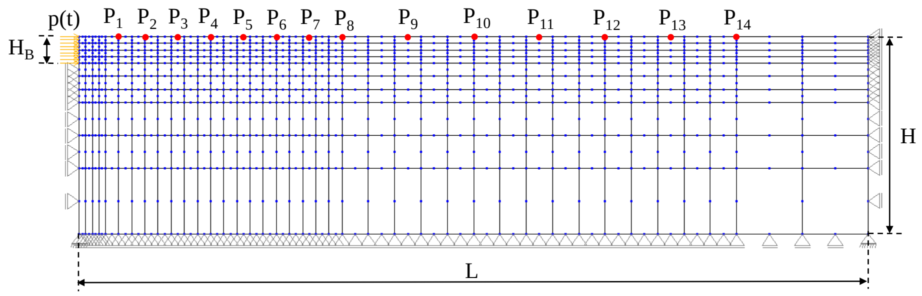


Fig. 5 Finite element mesh and boundary conditions at a limestone quarry.

The Newmark algorithm was used with values of 0.316 for α and 0.625 for δ. The total time evaluated was 0.3s, which showed sufficient time to reach 500m from the blasthole for the seismic wave produced by the detonation. The evolution of time took place in two blocks. The first block consists of 40 equal time increments of $5.0 \times 10^{-5}$s until the time instant of $2 \times 10^{-3}$s to be able to capture the pressure pulse variation over time. The second block comprises of 2980 equal time increments of $10^{-4}$s until the time instant of 0.3s. So, increasing the time increment it is possible to reduce computational cost.

The Rayleigh damping method, Eq. (6), was adopted to simulate the effect of physical damping, since it is a common practice in the context of elastic analysis in geomechanical applications. The natural frequencies ($\omega_i$ and $\omega_j$) selected for the calculation of $\alpha_R$ (Eq. 7a) and $\beta_R$ (Eq. 7b) were, respectively, 135.57 and 147.28rad/s. These correspond to the lower natural frequencies for the finite element mesh and material properties taken in this problem. Adopting the damping ratio as 2.5% (which correspond to the best fit of the numerical (by ANLOG) and field (by Toraño *et al.*, 2006) attenuation law), the Rayleigh coefficients ($\alpha_R$ and $\beta_R$) of 3.53 and $1.8 \times 10^{-4}$ are obtained. Still, a sensitive analysis was performed first by keeping constant the $\alpha_R$ value of 3.35 and varying the $\beta_R$ value and after that by keeping constant the $\beta_R$ value of $1.8 \times 10^{-4}$ and varying the $\alpha_R$ value.

Figure 6a shows that, while keeping the $\alpha_R$ value constant and increasing the $\beta_R$ value, PPV levels decrease. It is noted that the numerical results presents some characteristic noise for the smaller values of $\beta_R$ ($0.5x10^{-4}$ and $1.0x10^{-4}$). These noises are attenuated when the value of $\beta_R$ increases. It demonstrates that $\beta_R$ has the ability to damp the high frequencies of non-physical vibrations, that is, the noise derived from numerical simulation, as indicated by Cook et al. [16]. Figure 6b demonstrates that the $\alpha_R$ value affects vibration attenuation as the seismic wave moves away from the point of origin. It is observed that the vibration attenuation at distant points is more intense while keeping $\beta_R$ constant and increasing the $\alpha_R$ value.

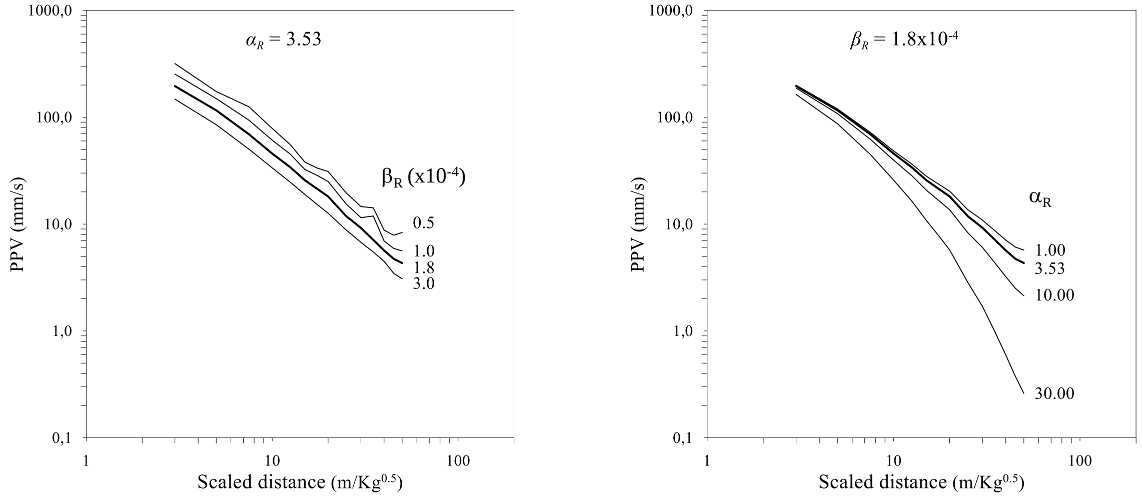


(a) Influence of $\beta_R$ on the attenuation curve. (b) Influence of $\alpha_R$ on the attenuation curve.

Figure 6: Numerical attenuation curves in function of the Rayleigh coefficients.

Knowing the influence of the Rayleigh coefficients on the results obtained, it is verified that the numerical attenuation law converges to the field attenuation law with the values of $\alpha_R$=10.0 and $\beta_R$=$1.1x10^{-4}$ (Toraño et al. [4]). Figure 7 shows the field attenuation curve and the results acquired by the Algor program reported by Toraño et al. [4], as well as the results obtained by ANLOG. In general, the numerical results obtained may be confirmed to be similar to those predicted by the attenuation law.

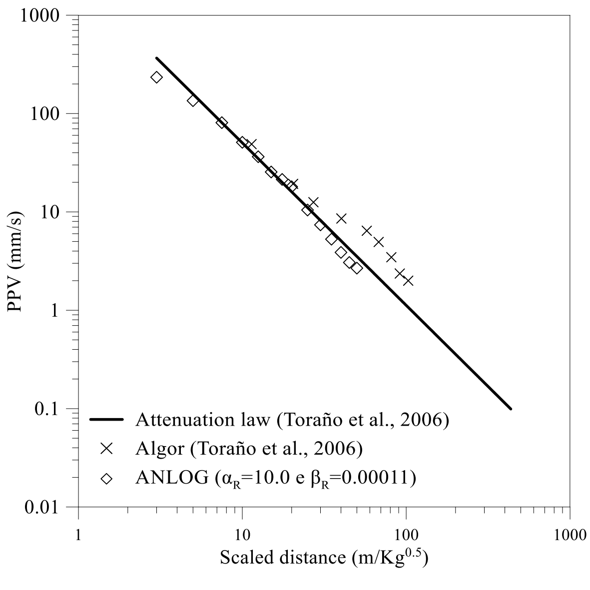


Figure 7: Attenuation law: ANLOG versus Algor.

# 4 Conclusions

The current study demonstrated the significance of dynamic stress-strain analysis in obtaining blast-induced ground vibrations. The results revealed the ANLOG program's capacity to perform individualized rock mass analysis under blast-induced dynamic stress, taking into consideration geological and geomechanical characteristics specific to each medium as well as blast parameters, at a reasonable speed and low cost. The application problem presented showed the importance of the Rayleigh coefficients on the numerical results.

**Acknowledgements.** This study was financed in part by the Coordenação de Aperfeiçoamento de Pessoal de Nível Superior - Brasil (CAPES) - Finance Code 001. The authors would like to thank CAPES, CNPq, FAPEMIG, Fundação Gorceix, PPGEM/UFOP, PROPEC/UFOP, and PROPP/UFOP for their financial support. The first author would like to thank CAPES for their grant.

**Authorship statement.** The authors hereby confirm that they are the sole liable persons responsible for the authorship of this work, and that all material that has been herein included as part of the present paper is either the property (and authorship) of the authors, or has the permission of the owners to be included here.

# References

[1] ABNT NBR 9365. Guia para avaliação dos efeitos provocados pelo uso de explosivos nas minerações em áreas urbanas. Rio de Janeiro, 2018.
[2] J. F. Semblat. Modeling seismic wave propagation and amplification in 1D/2D/3D linear and nonlinear unbounded media. *Int J Geomech*, 11, pp. 440–448, 2010.
[3] G. W. Ma, H. Hao, Y. X. Zhou. Modeling of wave propagation induced by underground explosion. *Computers and Geotechnics*, 22, pp. 283–303, 1998.
[4] J. Toraño, R. Rodríguez, I. Diego, J. M. Rivas, M. D. Casal. FEM models including randomness and its application to the blasting vibrations prediction. *Computers and Geotechnics*, 33, pp. 15–28, 2006.
[5] C. Jommi and A. Pandolfi. Vibrations induced by blasting in rock: a numerical approach. *Rev Ital Geotec*, 20, pp. 77–94, 2008.
[6] W. Lu, J. Yang, M. Chen, C. Zhou. An equivalent method for blasting vibration simulation. *Simulation Modelling Practice and Theory*, 19, pp. 2050–2062, 2011.
[7] K. Liu, H. Hao, X. Li. Numerical analysis of the stability of abandoned cavities in bench blasting. *Int J Rock Mech Min*, 92, p. 30-39, 2017.
[8] J. Xu, Y. Kang, X. Wang, G. Feng and Z. Wang. Dynamic characteristics and safety criterion of deep rock mine opening under blast loading. *Int J Rock Mech Min*, vol. 119, pp.156–167, 2019.
[9] C. B. Zorzal. Análise dinâmica via MEF das vibrações induzidas pelo desmonte de rochas. Master's thesis. Universidade Federal de Ouro Preto, 2019.
[10] C. J. Martins. Condições Iniciais em Propagação de Ondas Elásticas Através do Método dos Elementos Finitos nos Domínios do Tempo e da Frequência. PhD thesis, Universidade Federal do Rio de Janeiro, 2004.
[11] K. J. Bathe. *Finite Element Procedures*. Prentice-Hall Inc., 1996.
[12] R.W. Clough and J. Penzien. *Dynamics of structures*. Computers & Structures Inc., 2003.
[13] C. L. Nogueira. Análise não linear de escavações e aterros. PhD thesis, Pontifícia Universidade Católica do Rio de Janeiro, 1998.
[14] M. R. Saharan and H. S. Mitri. Numerical Procedure for Dynamic Simulation of Discrete Fractures Due to Blasting. *Rock Mech. Rock Engng.*, 41, pp. 641–670, 2008.
[15] A. K. Chopra. *Dynamics of structures*. Prantice-Hall, 2012.
[16] R. D. Cook, D. S. Malkus, M. E. Plesha, R. J. Witt. *Concepts and Apllications of Finite Element Analysis*. John Willeys & Sons Inc., 2001.